Integrated approach for modeling acoustic propagation and projectors/hydrophones electronics

Rúben Viegas*, Daniel Pozzatti†, Friedrich Zabel‡ and António J. Silva§
*LARSyS, Universidade do Algarve, Campus de Gambelas, 8005-139 Faro, Portugal
Email: a77916@ualg.pt
†Marsensing Lda, Centro Empresarial - Pav. A5, Campus de Gambelas, 8005-139 Faro, Portugal
Email: dpozzatti@marsensing.com
‡Marsensing Lda, Centro Empresarial - Pav. A5, Campus de Gambelas, 8005-139 Faro, Portugal
Email: fredz@marsensing.com
§LARSyS, Universidade do Algarve, Campus de Gambelas, 8005-139 Faro, Portugal
Email: asilva@ualg.pt

OCEANS 2022, Hampton Roads | 978-1-6654-6809-1/22/$31.00 ©2022 IEEE | DOI: 10.1109/OCEANS47191.2022.9977091

***Abstract*—Underwater acoustic propagation models (APM) are useful tools to predict acoustic propagation, making it possible to implement and test equalization algorithms for Underwater Acoustic Communication (UWAC) systems. To our knowledge, none of the APMs developed so far consider the distortion induced by the associated electronic circuits, impedance adaptors and acoustic transducers on signal propagation, which are important mainly in broadband applications. This paper describes the functioning of a new model capable of predicting the aforementioned distortions on the projector and hydrophone. The electro-Acoustic Propagation Model (eAPM) calculates the frequency response of the circuits with frequency-dependent characteristic components (transducers and impedance adaptors) using SPICE simulations and simulates the acoustic propagation using an Time-Variable APM (TV-APM), all embedded in a single model. SPICE simulations require the insertion of electrical impedance measurements from the transducers and impedance adaptors. eAPM also uses the projector's Transmitting Voltage Response (TVR) and the hydrophone's Open Circuit Voltage Response (OCVR), that can be obtained through equipment calibration. The model output signals have a good agreement with the signal experimentally recorded, showing that the eAPM allows for in-lab prediction of the distortion induced by the transducers and electronics and its impact on an application in a realistic acoustic propagation environment. The developed model can be used to predict distortions on broadband UWAC systems and also to support the development of new transducers, especially those with a wide bandwidth response.**

***Index Terms*—Acoustic Transducers, Acoustic Propagation Model, SPICE simulation, Impedance Adaptation, Transmitting Voltage Response, Open Circuit Voltage Response**

I. Introduction

Underwater acoustic propagation models (APM) are useful to predict acoustic propagation in a given environment, making it possible to implement equalization algorithms and test them in laboratory conditions. Currently, some APMs (Bellhop [1] and TRACEO [2], [3]) allow modeling the acoustic field considering the static conditions such as bathymetry and sound speed profile. There are also models that consider non-static conditions such as transmitter-receiver motion and surface waves, as is the case of Virtual Timeseries EXperiment (VirTEX) [4] and Time-Variable APM (TV-APM) [5] that are able to predict the Doppler channel spread. However, to our knowledge, none of the APMs developed to date considers the distortion induced by the associated electronic circuits and acoustic transducers on signal propagation.

In Underwater Acoustic Communications (UWAC), in addition to simulating the propagation of sound underwater, it is also important to simulate the electronic behavior of the associated equipment: projector (sound source) and hydrophone (sound receiver). The transducers present in the mentioned equipment have an impedance that varies with the frequency of the emitted/transmitted signal that can cause unexpected distortions in amplitude and phase, if are not considered the electronic properties of the equipment.

Currently, PiezoCAD software [6] is capable of electronically and acoustically simulate piezoelectric transducers. However, the absence of an integrated APM, makes it impossible to perform the electroacoustic simulation of systems as, e.g., for broadband communications.

This article describes the development of a tool capable of model simultaneously the acoustic propagation, and the electronic behavior of the projector and the hydrophone, making the simulation of UWAC systems more realistic.

II. Electronics and Transducers acoustic signal distortion

Transducers and the associated electronics for projectors and hydrophones induce frequency-dependent amplitude and phase distortion on the transmitted and received signals, respectively, which are usually ignored since most applications use very narrowband signals. However, for broadband applications like spread-spectrum or OFDM modulations, those distortions can no longer be ignored [7]. Those amplitude and phase distortions are primarily due to amplifiers' non-linearity, impedance adaptors, and transducer impedance, which can vary strongly with frequency.

Since the electronic properties of transducers vary with frequency, the electro-acoustic properties, Transmitting Voltage Response (TVR) and Open Circuit Voltage Response (OCVR), also depend on frequency. TVR and OCVR which consist on the ability to transform the electrical signal into sound and vice versa, are usually considered in terms of amplitude. However, its phase frequency dependence is relevant for broadband applications.

Figure 1a shows an acoustic transducer that has a frequency-dependent impedance (Z). One of the possibilities to represent and measure the transducer impedance is using its series equivalent model represented in Fig. 1b. This equivalent model is characterized by a capacity (C) and a resistance (R) in series. The impedance characteristics (C and R) can be obtained through LCR-meter measurements, and the acoustic characteristics (TVR and OCVR) can be obtained through equipment calibration.

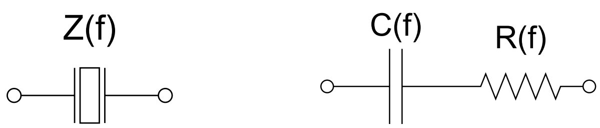

(a) (b)

Fig. 1: Transducer representation: (a) transducer circuit schematic and (b) the series equivalent model of the transducer.

The acoustic transducers are usually made of piezoelectric ceramics as PZT, and more recently of piezoelectric polymers, such as PVDF [8]. PVDF transducers are recommended for broadband applications due to their broad-resonance bandwidth [9], while PZT transducers are more suitable for narrowband applications due to their narrow-resonance bandwidth [10]. Figure 2a shows an example of a C/R plot, and Figure 2b shows a TVR plot, both of a multilayer PVDF acoustic projector. The phase term of TVR is usually not provided by the manufactures mostly because its frequency dependent shape results from the interaction between the transducer impedance and electronics being used on the equipment setting.

III. Electro-acoustic propagation model Development

The electro-acoustic propagation model (eAPM) consists of a MATLAB toolbox (Python version is being developed) that integrates the electrical and acoustic behavior, allowing to observe the changes of the electrical and acoustic signals in all steps of the transmitting/receiving system.

Figure 3 shows the eAPM block diagram where on top is represented the signal path from the input to the output and on the bottom the input data/information required by each block operation. On top: (i) the electrical signal $x'(t)$ crosses the electronic simulator (left red square in the figure) considering the projector transducer impedance; (ii) the TVR converts the electric signal to acoustic $x(t)$; (iii) TV-APM simulates the 'Sea' acoustic propagation; (iv) the received acoustic signal $y(t)$ is converted to electric signal (through the hydrophone OCVR); and (v) the electric signal crosses the electronic simulator considering the hydrophone transducer impedance and generates the received electric signal $y'(t)$. The eAPM requires: (i) the SPICE simulation of the projector electronics (schematics of amplifiers, filters, etc.) and the piezo-impedance characteristics measured with an LCR-meter; (ii) the projector-TVR estimated or measured during calibration; (iii) the information about the environment (bathymetry, sound speed profile, equipment position, etc.); (iv) the hydrophone-OCVR estimated or measured during calibration; and (v) the SPICE simulation of the hydrophone electronics (schematics of amplifiers, filters, etc.). It should be noted that the information about the transducers is split between the frequency-dependent electrical impedance (Fig. 2a) and electro-acoustic characteristics: the projectors-TVR (Fig. 2b) and hydrophones-OCVR.

[1]KEYSIGHT E4980A

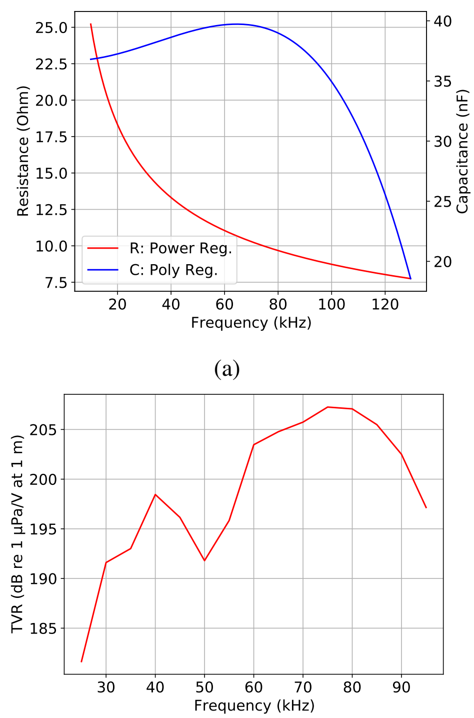

(b)

Fig. 2: Characteristics of a multilayer PVDF transducer: **(a)** Capacitance and Resistance regressions from the measured values with the LCR-meter[1]; **(b)** Transmitting Voltage Response obtained through an projector calibration.

In terms of the software approach, the model is divided into two parts: Acoustic Propagation Model and Electronic Circuits Simulation.

A. Acoustic Propagation Model

The APM used in this work is the TV-APM [5], which automatically executes the ray tracing model Bellhop [1]. Another APM could have been used, providing the ability to generate the impulse response (IR) of the acoustic channel, with the simulation bandwidth validation.

The TV-APM inputs are the signal bandwidth and the static and variable environmental parameters as is the case

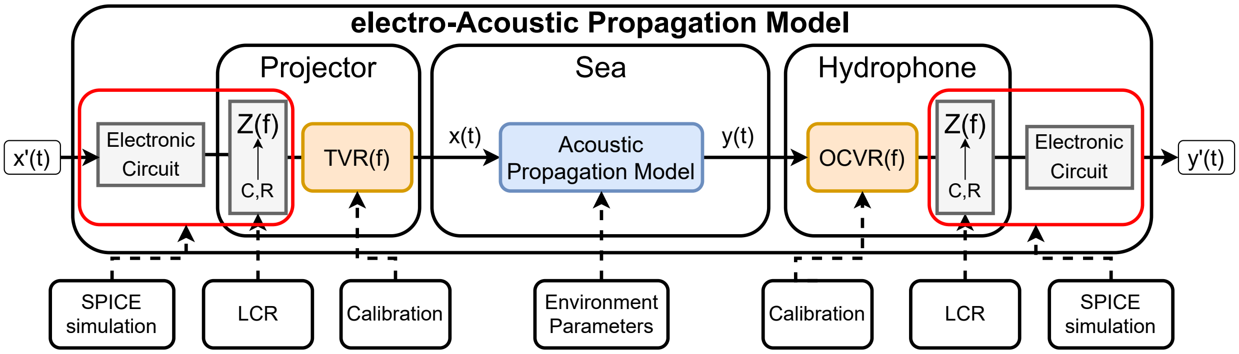

Fig. 3: Block diagram of the electro-Acoustic Propagation Model (eAPM): the electric signal $x'(t)$ crosses the electronic simulator considering the projector transducer impedance; the TVR converts the signal to acoustic $x(t)$; APM simulate its propagation; the received acoustic signal $y(t)$ is converted to electric signal (through the OCVR) that crosses the electronic simulator, considering the hydrophone transducer impedance, and generates the received electric signal $y'(t)$.

of bathymetry and the position of the equipment (Fig. 4a), and the output is the time-variable IR h_{APM} which is used to calculate the output signal of a given system, based on the input signal [5]. Since TV-APM is capable of simulating time-variable scenarios, the IR generated is delay-dependent as shown in Fig. 4b, and the output signal calculation is given by the time-variable convolution

$$y(t) = \int x(t-\tau) h_{\text{APM}}(t,\tau) d\tau \tag{1}$$

from [5, eq. 7]. Otherwise, the calculation becomes simpler and is given by

$$y(t) = x(t) * h_{\text{APM}}(t) \Leftrightarrow Y(f) = X(f) H_{\text{APM}}(f), \tag{2}$$

where $H_{\text{APM}}(f)$ represents the Fourier transform of the IR, also named frequency response (FR).

B. Electronic Circuits Simulation

An electronic circuit that has transducers and impedance adaptors with frequency-dependent characteristics can be modeled with an electronic SPICE simulator such as LTspice [12], which is the software used in the eAPM. When the goal is to simulate the circuit FR, the LTspice AC analysis is the usual approach. Since the AC analysis does not allow to vary the characteristics of the components with the frequency of the input signal, several transient analyses have to be used. The capacitance and resistance values are introduced into the SPICE-directive of LTspice by the regression of the LCR-meter measured values. Then, LTspice performs several SPICE transient analyses in the background, varying simultaneously the frequency of the input sinusoid (f_i) and the characteristics of the transducer (that depend on f_i). Listing 1 shows an SPICE-directive example of 21 SPICE transient analyses that can be used to study circuits with frequency-dependent characteristics.

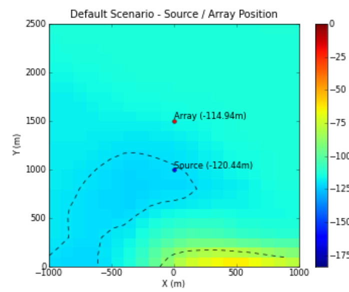

(a)

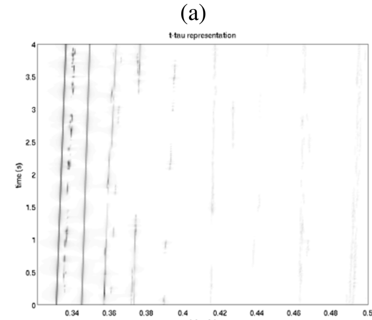

(b)

Fig. 4: TV-APM: example of (a) bathymetry and equipment position; (b) time-variable IR with Doppler spread due to surface waves and transmitter-receiver motion [11].

```
.tran 0 20m 0
.step param FI 15k 100k 4.25k
.param R = (1.7554e3)*pow(FI,-4.6067e-1)
.param C = ((2.4923e-18)*(FI**2))+...
```

Listing 1: SPICE-directive example: 20 ms simulation; signals from 10 to 100 kHz with an 4.25 kHz increment; R and C are frequency-dependent functions.

In this work, the approach was to generate the circuit FR to be used with broadband signals. Since we are using transient analysis, it is necessary to analyze the output signal of the circuit ($s_{out}(t)$) for a giving set of sinusoidal inputs ($s_{in}(t)$) covering the frequency band of interest. This allows to compute the one-sided FR

$$H_{OS}(f) = A(f)e^{i\phi(f)}. \tag{3}$$

where $A(f)$ and $\phi(f)$ are the gains and phase differences for each frequency, f_i, respectively.

The described method was carried out for an acoustic projector circuit ($H_P(f)$) and for the hydrophone circuit ($H_H(f)$) used in section IV. In case the simulation time is too high due to the assembly of multiple sub-circuits in series, it is recommended to simulate the sub-circuits separately and multiply all FR's.

C. electro-Acoustic Propagation Model

The eAPM uses the acoustic channel IR or FR (section III-A), the circuits FR's (section III-B), projector-TVR and hydrophone-OCVR to calculate the electric and acoustic signals generated from the input to the output of the system in Fig. 3. In such context, the transmitted acoustic signal $x(t)$ in the frequency domain is given by

$$X(f) = X'(f)H_P(f)H_{\text{TVR}}(f), \tag{4}$$

the received acoustic signal $y(t)$ is given by equation 1 or 2 for time-variable or static scenarios, and the output electrical signal $y'(t)$ is given by

$$Y'(f) = Y(f)H_{\text{OCVR}}(f)H_H(f). \tag{5}$$

The $H_{\text{TVR}}(f)$ and $H_{\text{OCVR}}(f)$ calculation consists of the same method used for the calculation of $H_P(f)$ and $H_H(f)$, described in section III-B.

Considering a static scenario, the global IR of the channel is given by

$$H(f) = H_P(f)H_{\text{TVR}}(f)H_{\text{APM}}(f)H_{\text{OCVR}}(f)H_H(f). \tag{6}$$

For reducing the time required for the simulations the eAPM can be executed with the signals and FR's in baseband. The use of eAPM for systems with multiple sources and/or multiple receivers is possible with the same rationale but the execution time increases.

IV. Model Validation

In order to validate the developed eAPM, an practical experiment was made in April 21, 2022 at Ria Formosa Lagoon, in Faro, Portugal. The objective of the experiment was the calibration of an PVDF projector [13], using the setting represented in Fig. 5 for recording the required electric signals. The signal from the signal generator (S. G.) passes through a bandpass filter that is connected to the projector: two power amplifiers connected to an impedance adaptor and a multilayer PVDF transducer. The acoustic signal produced by the projector is received by a factory calibrated TC4033 hydrophone (PZT transducer), that is connected to its pre-amplifier. The signal is recorded at the two channels of the Data Acquisition system (DAQ CH1 and DAQ CH2), which corresponds to the input and output signals. Both acoustic equipment were placed 1 meter from the surface, 4 meters from the seabed, and 0.85 meters from each other horizontally. The bandpass filter function is to convert step-based sinusoids from the signal generator into pure sinusoids.

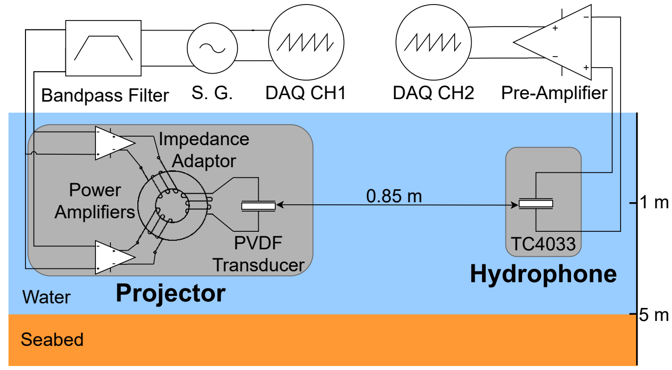

Fig. 5: Signal recording setting scheme: signal generator (S. G.), bandpass filter, projector (two power amplifiers, impedance adaptor, and multilayer PVDF transducer), TC4033 hydrophone and its pre-amplifier. The signal recording takes place at the two channels of the Data Acquisition system (DAQ CH1 and DAQ CH2).

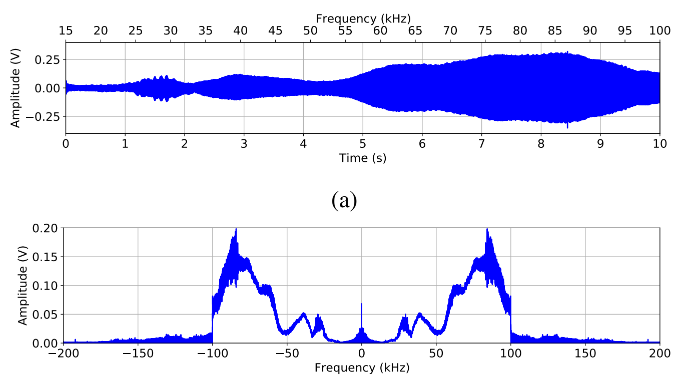

(a)

(b)

Fig. 6: Recorded signal, with $f_S = 400$ kHz: (a) time representation and (b) frequency representation.

The signal generated by the signal generator consisted of a 15-100 kHz linear up-chirp with 0.25 V constant amplitude. Figure 6 shows the time and frequency representation of the recorded signal at DAQ CH2, showing the signal noise and the frequency-dependent amplitude distortion induced mainly by the acoustic equipment, as it is a short-distance underwater propagation without multipath.

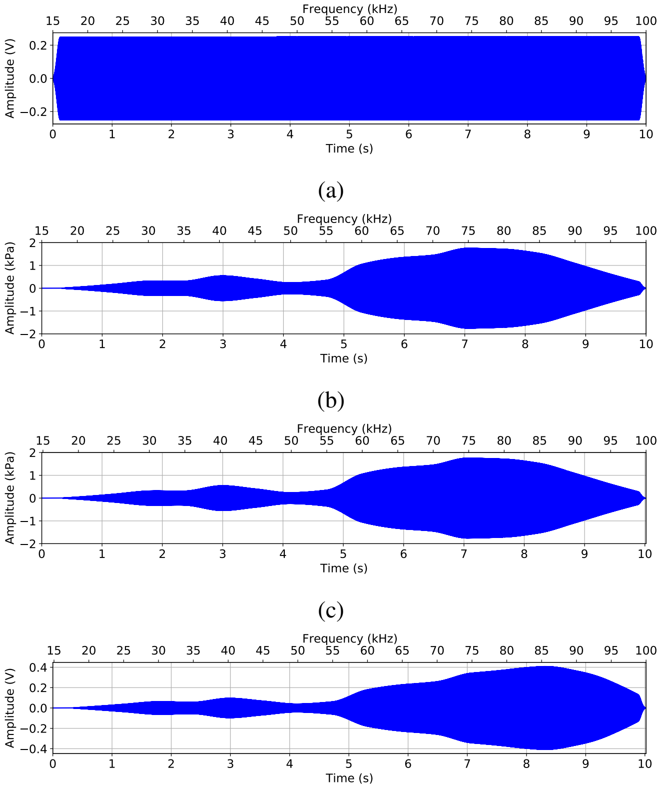

(a) (b) (c) (d)

Fig. 7: Time representation of the eAPM simulated signals, with $f_S = 400$ kHz: (a) input electrical signal $x(t)$, (b) input acoustic signal $x'(t)$, (c) output acoustic signal $y'(t)$, and (d) output electrical signal $y(t)$.

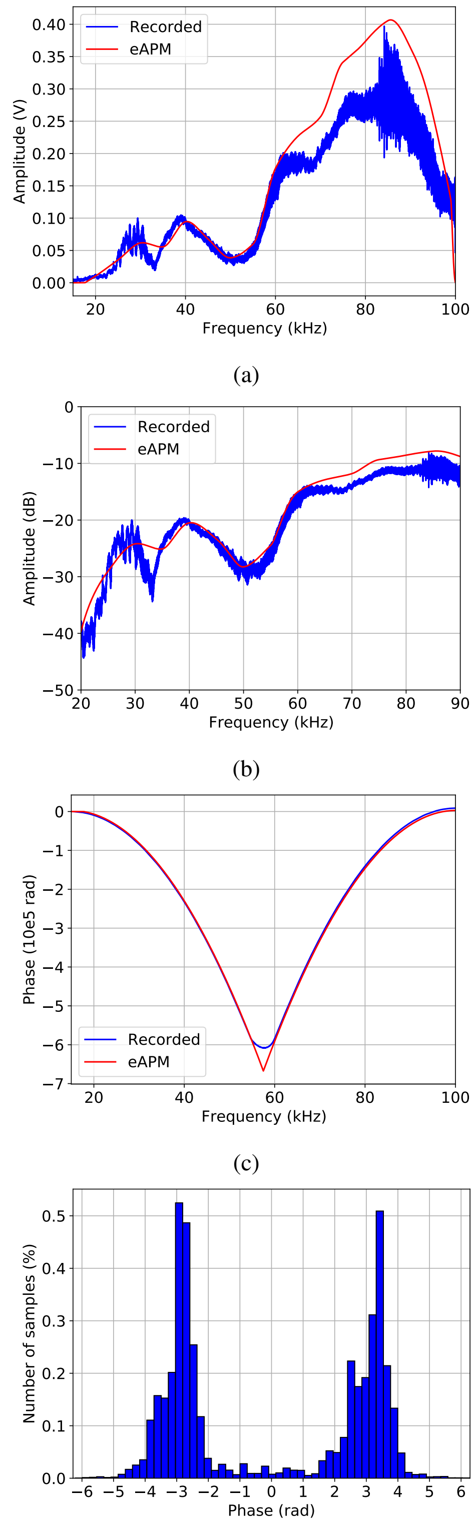

(a) (b) (c) (d)

Fig. 8: Signal comparison: recorded and eAPM amplitude values depending on the frequency, in (a) volts and (b) decibels; (c) recorded and eAPM unwrapped phase values depending on the frequency; (d) histogram of wrapped phase difference values.

When running eAPM with the respective data (TVR, OCVR, circuits, impedance values, and environment parameters), it outputs the signals represented in Fig. 7: $x(t)$, $x'(t)$, $y'(t)$ and $y(t)$ from Fig. 3. It is possible to observe the signal change in the various steps of the UWAC system. The output electrical signal $y(t)$ (Fig. 7d) represents the eAPM simulation of the recorded signal (Fig. 6), making it possible to compare them.

Figure 8 shows the amplitude and phase comparison between the recorded signal and the eAPM simulated signal. Regarding the amplitude values in Figs. 8a and 8b for linear and dB scales, respectively, the curves have similar shapes and the same order of magnitude, however with a maximum difference of approximately 3 dB at high frequencies.

Figure 8c shows that the unwrapped phase curves have the same curve shape, except in the 58 kHz region. Figure 8d shows the histogram of the phase [14], where it gets clear that there are two most frequent phase difference values near $-\pi$ and π radians.

Analyzing the obtained amplitude results (Fig. 8b) it is possible to observe that eAPM has an error of up to 2.5 dB at 80 kHz that may be due to some SPICE simulator miscalculation, and that for most frequencies it is negligible. Regarding the phases shown in Fig. 8d, the phase difference is approximately 180° which is possibly due to the phase inversion of the hydrophone pre-amplifier at the receiver side. Figure 8d does not have two well defined peaks due to the noise present in the recorded signal which affects the phase of the entire signal spectrum.

V. Conclusion

The development of the electro-Acoustic Propagation Model (eAPM) arises from the need to predict in-lab not only acoustically but also electroacoustically the signals in UWAC systems, since, in broadband applications, distortions and misfits may occur in the signals that the APMs could not predict.

The developed eAPM consists on the integration in a single model, an APM, an electronic SPICE simulator, and the transducers characteristics (the projector-TVR, the hydrophone-OCVR and transducer impedance measurements). The eAPM is capable of simulating electrical and acoustic signals in the all system steps: inside the electronic and acoustic subsystems. Or, in other words, the inputs and outputs of electronic components and inputs and outputs of acoustic parts.

The model validation (comparison between the eAPM and the recorded signals) shows that the performance of the eAPM is good for predict the electronic and acoustic signals on broadband UWAC systems. The eAPM was and can also be used to support the development of new transducers, especially with a wide bandwidth resonance.

For future work, it will be important to study in detail the performance and simulation of impedance adapters, as well as carry out more validation tests with more recordings of practical experiences. The eAPM will be available for free use on the SiPLAB website (http://www.siplab.fct.ualg.pt/).

VI. Acknowledgement

This work was supported by the Project OceanTech - Sistema de Gestão de Operacões com base em Veículos Robóticos Inteligentes para a Exploração do Mar Global a partir de Portugal, POCI-01-0247-FEDER-024508 - funded by FEDER funds through the Operational Program for Competitiveness and Internationalization (COMPETE2020); and the project K2D: Knowledge and Data from the Deep to Space with reference POCI-01-0247-FEDER-045941, cofinanced by the European Regional Development Fund (ERDF), through COMPETE2020, and by the Portuguese Foundation for Science and Technology (FCT) under the MIT Portugal Program.

References

[1] M. B. Porter and H. P. Bucker, "Gaussian beam tracing for computing ocean acoustic fields," *The Journal of the Acoustical Society of America*, vol. 82, no. 4, pp. 1349–1359, Oct. 1987.

[2] O. Rodríguez, *The TRACEO ray tracing program*, Physics Department, SiPLAB, FCT, University of Algarve, 2011. [Online]. Available: http://www.siplab.fct.ualg.pt/models/traceo/manual.pdf

[3] O. C. Rodríguez, J. M. Collis, H. J. Simpson, E. Ey, J. Schneiderwind, and P. Felisberto, "Seismo-acoustic ray model benchmarking against experimental tank data," *The Journal of the Acoustical Society of America*, vol. 132, no. 2, pp. 709–717, Aug. 2012.

[4] M. Siderius and M. B. Porter, "Modeling broadband ocean acoustic transmissions with time-varying sea surfaces," *The Journal of the Acoustical Society of America*, vol. 124, no. 1, pp. 137–150, Jul. 2008.

[5] A. Silva, O. C. Rodríguez, F. Zabel, J. Huillery, and S. M. Jesus, "Underwater acoustic simulations with a time variable acoustic propagation model," in *Proc. 10th European Conference on Underwater Acoustics*, Istanbul (Turkey), Jul. 2010.

[6] Sonic Concepts, Inc, "Piezocad." [Online]. Available: https://sonicconcepts.com/software/

[7] T. Xu and L. Xu, *Digital Underwater Acoustic Communications*. New York, NY, USA: Academic Press, 2017.

[8] S. C. Butler, "Properties of transducers: underwater sound sources and receivers," Naval Undersea Warfare Center Division Newport United States, Tech. Rep., 2018.

[9] K. Uchino, "Introduction to piezoelectric actuators and transducers," Pennsylvania State University: University Park, PA, USA, Tech. Rep., 2003.

[10] T. Necsoiu, I. Chilibon, M. Robu, V. Cătuneanu, and A. Stan, "Some aspects of the piezoceramic materials utilized in sensitive hydrophones," *Sensors and Actuators A: Physical*, vol. 60, no. 1-3, pp. 139–141, 1997.

[11] O. Rodríguez, A. J. Silva, F. Zabel, and S. M. Jesus, "The TV-APM interface: a web service for collaborative modelling," in *Proc. 10th European Conference on Underwater Acoustics*, Istanbul (Turkey), Jul. 2010.

[12] Analog Devices, Inc, "Ltspice." [Online]. Available: https://www.analog.com/en/design-center/design-tools-and-calculators/ltspice-simulator.html

[13] A. Silva, A. Hughes, D. Pozzatti, F. Zabel, R. Viegas, and M. S. Martins, "Development of a high-power multilayer PVDF acoustic projector for 50 to 80 khz band," 2022, to be presented at OCEANS 2022 Hampton Roads.

[14] Q. Tan, A. Yang, and P. Guo, "Blind modulation format identification using differential phase and amplitude ratio," *IEEE Photonics Journal*, vol. 11, no. 1, pp. 1–12, Feb. 2019.